IEEE Access
Multidisciplinary ⋮ Rapid Review ⋮ Open Access Journal

Received 10 December 2024, accepted 8 January 2025, date of publication 15 January 2025, date of current version 24 January 2025.

Digital Object Identifier 10.1109/ACCESS.2025.3530145

RESEARCH ARTICLE

Development of a Multi-Sensor Mobile Device for Urban Air Quality Monitoring at the Street Corner: The SMILE Project

JONAS PELLEGRINO[1], (Student Member, IEEE), HASSEN AZIZA[1], (Member, IEEE), MATHIEU GUERIN[1], (Member, IEEE), PASCAL TARANTO[1], (Member, IEEE), WENCESLAS RAHAJANDRAIBE[1], (Member, IEEE), AND BLAISE RAVELO[2], (Senior Member, IEEE)

[1]Aix-Marseille University, CNRS, University of Toulon, IM2NP UMR7334, 13007 Marseille, France
[2]School of Electronic and Information Engineering, Nanjing University of Information Science and Technology (NUIST), Nanjing, Jiangsu 210044, China

Corresponding author: Jonas Pellegrino (Jonas.pellegrino@im2np.fr)

This work was supported by the SMILE Project which was approved by the French National Centre for Scientific Research (CNRS) Committees and funded on a research and innovation call in 2020–2022 for a Proof of Concept by (DARII) "Région-Sud" (Division of the South Region, France), the SATT-SE "Technology Transfer Office of Southeast" and the Mission for Transverse and Interdisciplinary Initiatives (MITI), CNRS.

ABSTRACT Air pollution is a critical contributor to the global climate change crisis and poses severe threats to human health worldwide. In this context, this paper introduces an innovative multi-sensor air quality monitoring (AQM) device designed to address the critical challenge of atmospheric pollution in urban environments. The AQM device features an optimized geometry specifically suited for mobility. It enables precise air quality (AQ) monitoring by measuring concentrations of NO_2, O_3, and CO, along with particulate matter (PM) across three size categories: PM1, PM2.5, and PM10. The AQM device ensures reliable operation across temperature variations from 10°C to 40°C and humidity levels ranging from 10% to 70%. Outdoor experiments were conducted in the city of Marseille to validate the efficiency of the AQM device and assess its ability to provide street-level air quality data. The AQM device was validated by comparing its measurements with data from four reference instruments (i.e., government-operated fixed stations) located within an 8 km radius of the center of Marseille. Real-time data is made available through a dedicated software server platform, offering geo-localized air quality information and detailed reports. The developed device offers excellent autonomy, with a full battery discharge lasting up to 28 hours, allowing it to be used throughout an entire day without the need for recharging. The proposed multi-sensor device was developed in the scope of the SMILE project (Self-calibrating air pollution Multi-sensors and ICDT platform to Leverage citizen's Empowerment). The project aims to empower end users with the responsibility of carrying, activating, and monitoring their own sensor devices while utilizing specialized apps on their mobile phones.

INDEX TERMS Air quality, citizen's empowerment, monitoring system, network, sensor.

I. INTRODUCTION

Since pollutants that may be present in the air have a direct impact on people's health and climate change [1], [2], [3], air quality has become a major concern. Thanks to increasing public awareness and easier access to information, both municipalities and citizens are becoming more interested in improving air quality (AQ) [4]. Facilitating access to a mobile AQ monitoring device that is affordable, accurate, and easily transportable could play a key role in educating citizens about the importance of AQ [5], [6].

The associate editor coordinating the review of this manuscript and approving it for publication was Stefano Scanzio.

Traditionally, AQ monitoring relies on static measurement units made of expensive and complex reference instruments [7]. These static measurement systems are usually larger, more energy-consuming and more expensive compared to mobile systems. A reference instrument is typically defined as a device certified by an official regulatory body and aligned with a reference method recognized in legal standards [7]. For instance, instruments to measure air pollutants for regulatory compliance purposes must be approved by the Environmental Protection Agency (EPA) for use in the USA or nominated for type testing according to the European Committee for Standardization (CEN) for use in the European Union. Reference instruments measure specific air pollutants to predefined criteria, such as precision, accuracy, drift over time, among others [8], to provide data that meets regulatory requirements. These AQ reference data [9] can have validity in courts of law. However, even though these static reference stations are highly accurate, their remoteness [10] could not permit to map AQ at the street level. In this context, this article proposes the design of a mobile AQ monitoring device [11] able to provide personalized environmental information at a micro-scale (street level) leveraging a network of low-cost sensors deployed across a specific area.

Mobile AQ devices are usually made of an integrated system that comprises one or more sensor sub-components and other supporting components needed to create a fully functional, autonomous and connected measurement device [8], [9], [10], [11], [12], [13], [14], [15], [16], [17]. The deployment of these mobile systems [12] is pushed by recent developments in both microelectronics and wireless technologies which has enabled the rise of small, ''low cost'' and energy-efficient devices that that can be organized into networks [5], [10], [11], [12], [18], [19], [20], [21], [22], [23], [24], [25], [26]. In the scope of this work, a ''low-cost'' mobile sensor refers to the initial purchase cost of a single functional sensor system when compared to the purchase cost of a single reference instrument measuring the same or similar atmospheric parameter(s). A sensor system is considered ''low-cost'' if the price of such a system is 100X orders of magnitude lower than a comparable reference instrument. Based on this new generation of mobile sensors, AQM can now be achieved using readily deployable low-cost devices, transforming the way environmental pollution is approached. In the last few years, many projects involving dense low-cost sensor networks deployed in the field have emerged to better understand the spatial variability of air pollution, in particular within the Smart City trend [11], [12], [25], [27], [28]. The approach adopted in this work follows the approach adopted in the previous projects by leveraging a Wireless multi-sensor Network (WSN) where each citizen could use a low-cost mobile device as a wearable for AQM. The proposed device is used in combination with a cell phone to communicate its measurements via Bluetooth low energy (BLE) protocol. The cell phone relays measured data to dedicated servers via the different cell phone data communication protocols (Wi-Fi, EDGE, 3G or 4G) [29]. Regarding the targeted pollutants, the proposed device considers the following pollutants: (i) Reactive gases including NO_2, O_3, CO and (ii) particulate matter (PM) in various size classes. The Air Quality Index (AQI) is also directly provided by the device.

Although the deployment of mobile sensors is within technical reach, important issues remain to be addressed. Recent scientific literature shows that the integration of different sensors in an IoT device at an affordable cost and under specific energy consumption constraints remains a challenge [5], [7]. In particular, the choice of sensors significantly impacts the battery lifetime. Moreover, selecting low-power sensors and optimizing operational parameters, such as sampling frequency (i.e., how often the sensors take measurements), can significantly extend battery life. Also, identical sensors may report measurement values differently, hence, sensor-to-sensor variations need to be evaluated accurately before deployment. On top of that, real-time, geo-localized and high-resolution AQ data need to be guaranteed for better decision-making and public awareness. In this context, the main contributions of this work are:

- The development of a low-cost, low-power, connected sensing device integrated with a mobile application for air quality monitoring.
- The development of a collaborative server-side platform for data visualization and sharing.
- The evaluation of the system's ability to measure, analyze, and report data in real-time for a specific area and across various use cases.

The remainder of this paper is organized as follows: Section II describes the AQM device design and implementation at the hardware level. Section III focuses on the software level implementation of the AQM device. Section IV presents the experimental calibration and validation of the multi-sensor device before deployment with a focus on sensor-to-sensor variations. Section V is dedicated to a real urban environment experimentation (city of Marseille) and provides a benchmark of the device performances versus state-of-the-art AQ sensors. Section VI discusses the social impact of the proposed solution. Finally, Section VII concludes the paper.

II. HARDWARE LEVEL IMPLEMENTATION

A. AQM DEVICE DESIGN

Fig. 1(a) presents the AQM device prototype along with its embedded sensors and supporting components (battery, USB charger, microcontroller with its integrated BLE antenna, Flash memory, etc.). The developed AQM device is powered by two 1-Ah Lithium Polymer batteries compliant with the device form factor, facilitating the device integration into its case (Fig. 1(b)). In addition to the rigorous selection of sensors, the project places significant emphasis on user-friendliness [21] as shown in Fig. 1(b) where a cloud-shaped prototype case housing the device is presented.

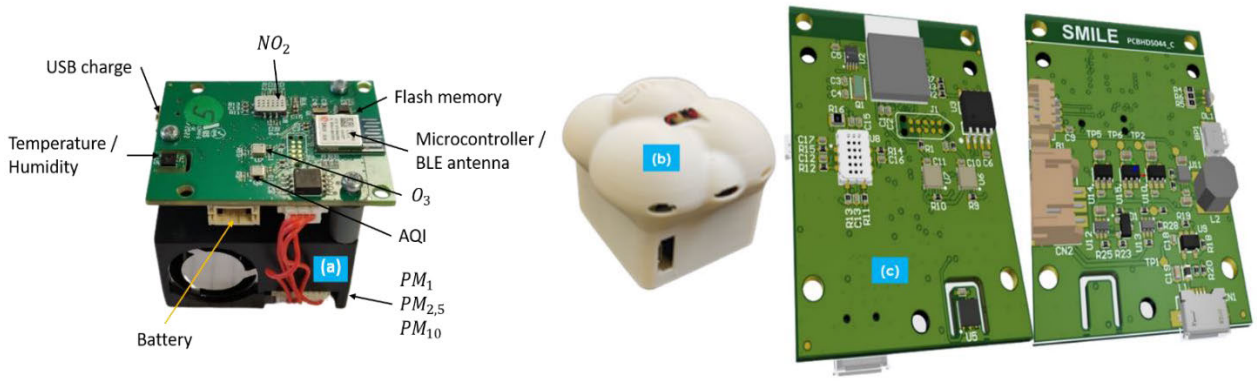

FIGURE 1. (a) Prototype of the SMILE device, (b) enclosure design concept and (c) 3D visualization of the double-sided electronic board featuring a 35 mm × 47 mm form factor.

This ergonomic design is intended to facilitate practical usage in both indoor and outdoor configurations. The designed enclosure ensures ease of handling and placement, allowing its integration into urban furniture (“street corners”). The device is combined with a mobile application to promote intuitive operation, making it accessible to a wide range of users (i.e., mobile application download), including citizens and city officials. Cost-effectiveness and compacity of the device have been improved by the design of a custom double-sided electronic board (Fig. 1(c)). The different modules constituting the AQM device are specified in the following subsection.

B. AQM DEVICE SPECIFICATIONS

Before the design stage, several critical requirements have been defined to ensure the proper operation of the system [30]:

1. Temperature range: The device is designed to operate at temperatures of up to 40°C, ensuring it can withstand different temperature conditions.
2. Form factor: The device’s Printed Circuit Board (PCB) form factor has been constrained to a compact 35 mm × 47 mm size to facilitate its deployment.
3. Power source: The device is designed to be powered by a rechargeable battery, ensuring its autonomy and mobility for urban deployment.
4. Cost-effectiveness: Maintaining an affordable cost for the multi-sensor device is crucial, and it has been designed to be priced under $90 to ensure its accessibility.

During the multi-sensor mobile device design, a particular emphasis has been placed on the reliability of all its components. The elementary sensors were carefully chosen to meet one of the main constraints of the device specifications, namely the power consumption. The target minimal operating time has been set to 12 hours without interruptions and with all sensors activated.

C. AQM DEVICE MODULE CHOICE STRATEGY

Table 1 shows a comparison of the main components of the AQM device (column 3) against similar items in terms of price and specifications (column 4). The following items have been considered:

- BMD-360: This is the integrated, low-energy MCU that supports BLE communication [31].
- MX25R6435F: This 64Mb flash memory has been chosen to record various configuration parameters and measurement data [32].
- MICS6814: This sensor measures nitrogen dioxide (NO_2) and carbon monoxide (CO) concentrations [33].
- PM3015: This sensor detects microparticulate matter that can impact AQ [34].
- ZMOD4510: This sensor is employed to monitor ozone (O_3) concentration and to determine the Air Quality Index (AQI) [35].
- Si7006: This sensor is responsible for capturing temperature and humidity changes, ensuring that environmental conditions are properly sensed [36].

D. AQM DEVICE ENCLOSURE DESIGN

The geometric analysis of the developed AQM sensor was conducted using a modeling tool during the prototyping phase. During this stage, the constituent material was meticulously selected to ensure the AQM device is protected against static electricity discharges. The enclosure was designed to allow heat dissipation without reducing the sensor’s performances. For the mobile version, the proposed shape is designed to avoid sharp edges so as not to hurt the user (see Fig 1b). The production of a mini-series of 250 sensors was carried out with respect to DFMA (Design For Manufacturing and Assembly [37]). Molten wire additive manufacturing was used to prototype a case that will be submitted to future users for feedback. After incorporating aesthetic elements (e.g., labels) and geometric adjustments, additive manufacturing [38] was employed to create a mass-production-ready

TABLE 1. Specification and cost comparison of Si7006, MICS6814, ZMOD4510 and PM3015 sensors.

Module	Specification	BMD-360	Ophelia-I
MCU for BT=BLE 5.1	Size	14x9.8x1.9 mm	7x9x2 mm
	Interfaces	SPI, UART, I2C, GPIO, PWM, PDM	UART, SPI, I2C, ADC
	Processing	64 MHz Arm Cortex-M4 processor	64 MHz Arm Cortex-M4 processor
	Memory	192 kB Flash, 24 kB RAM	192 kB Flash, 24 kB RAM
	Consumption	0.3 µA sleep, 7 mA transmit, 4.6 mA receive	0.3 µA sleep, 9.3 mA transmit, 6.8 mA receive
	Radio	Output power=4 dBm, Sensitivity=-97 dBm	Output power=4 dBm, Sensitivity (@50 Ω)=-93 dBm
	Price	4.80 €	9.27 €
Flash mem	Specification	MX25R6435F	S25FL064LABMFI013
	Size	4.1x4.1x0.6 mm	8x5.28x0.19 mm
	Interfaces	SPI	SPI
	Memory	64-Mb	64-Mb
	Life-span	100 000 Cycles and 20 years retention	100 000 Cycles and 20 years retention
	Clock rate	33 MHz	108 MHz
	Consumption	Read 6.5 mA, Program 10 mA for 33 MHz, 9 mA for 80 MHz read	Read 20 mA, Program 17 mA for 108 MHz, 10 mA for 50 MHz read
	High performance mode	Up to 320 MHz fast read	Up to 108 MHz
	Price	1.64 €	2.79 €
CO/NO_2 sensor	Specification	MICS-6814	MICS-4514
	Detected Gas	CO, NH3, NO_2, and various hydrocarbons	CO et NO_2
	Size	5 mm x 7 mm	5 mm x 7 mm
	Consumption	33mW	40mW
	Price	7 €	10,76 €
PM	Specification	PM3015	HPMA115C0-004
	Detection	PM1, PM2.5, PM10	PM1, PM2.5, PM4.0, PM10
	pm1, pm2,5	0~35µg/m3, ±5µg/m3	PM2.5: ±15 µg/m3; PM1.0, PM4.0, PM10: ±25 µg/m3 (0 µg/m3 to 100 µg/m3)
	pm1, pm2,5	>35µg/m3, ±15% of reading	
	pm10	0 ~100µg/m³, ±30 µg/m³	PM2.5: ±15 %; PM1.0, PM4.0, PM10: ±25% (100 µg/m3 to 1000 µg/m3)
	pm10	101 ~1000µg/m³, ±30% of reading	
	MTTF	37,297 hrs	87600 hrs
	Size	42×35×23.7 mm	44 mm x 36 mm x 12 mm (for compact)
	Consumption	working 100mA, standby 20mA	Inrush current 600mA, Supply current 80mA, standby current 20mA
	Price	16 €	77 €
O_3/AQI sensor	Specification	ZMOD4510	110-4xx
	Detected Gas	NO_2 (non-selective) O_3 (selective and non-selective depend on mode)	Ozone
	Range	20 to 500 ppb (ozone) 0 to 500 AQI	0 to 10 ppm
	AQI	±50	-
	Ozone	±8%	2%
	MTTF	proven over 15 years (5 years tested)	Over 10 years
	Size	3x3x0.7 mm	20x20x3 mm
	Consumption	0.2 mW	50 µW
	Price	8.38 €	18.39 €
Temp / HR sensor	Specification	Si7006-A20	Si7021-A20
	Temp	± 1 °C	± 0,4 °C
	HR	± 5 %	± 3%
	MTTF	10 years	10 years
	Size	3x3x0.75 mm	3x3x0.75 mm
	Consumption	60 nA standby, 150 µA Active	60 nA standby, 150 µA Active
	Price	2.5 €	7.95 €

enclosure to validate the constraints associated with IP (Ingress Protection) & IK (Impact Resistance) standards.

III. SOFTWARE LEVEL IMPLEMENTATION

Whether it is the mobile application or the server interface, creating a visually pleasing and user-friendly interface is essential. The latter bridges the gap between complex technology and everyday users, ensuring that monitoring and improving AQ in urban areas is a task that can be undertaken by all [28], [29], [39]. The software environment around the sensing device takes the form of a mobile application, which serves as an intermediary between the device and the data processing server, as depicted in Fig. 2.

A. MOBILE APPLICATION

The mobile application is the central component of the AQM system, serving as the interface between the users and the portable monitoring device. The mobile application enables

users to activate or deactivate specific sensors to suit their needs and select specific measurement parameters (such as the capture period) for the different sensors as shown in Fig. 3(a). Moreover, the application has been designed to maintain a stable BLE connection with the mobile device, ensuring smooth data transmission and user experience. The Flutter reactive BLE library [40] was chosen for its stability.

B. DATA SERVER

The server infrastructure is responsible for storing, managing, and facilitating access to the data collected from the portable monitoring device. The server was developed according to the following specifications:

- **Data Storage and Scalability**: The server, designed to retrieve, store, and process data over time, is equipped with high-throughput connectivity and large storage capacity. The server also provides scalability to accommodate increasing volumes of data.
- **Authentication and Authorization**: An authentication and authorization system has been implemented to regulate user access to specific data sets (e.g., access to a single user or multiple users' data, access to a single gas or multiple gases, access to specific areas, etc.) and maintain security.
- **Data Visualization**: The server offers different data visualization options, including displaying data on maps or in tabular form. Additionally, users can sort, and filter data based on various criteria to facilitate data analysis. The filtering can target specific gas, specific sensor devices, or a specific period. Fig. 3(b) presents

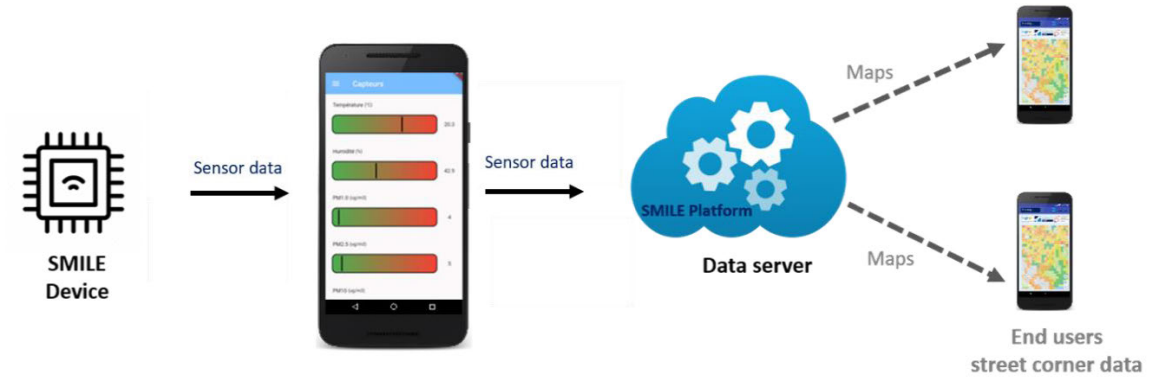

FIGURE 2. Sensing device (SMILE device) and data transmission through the mobile application to the data server. Request to the data server provide air pollution street-level information.

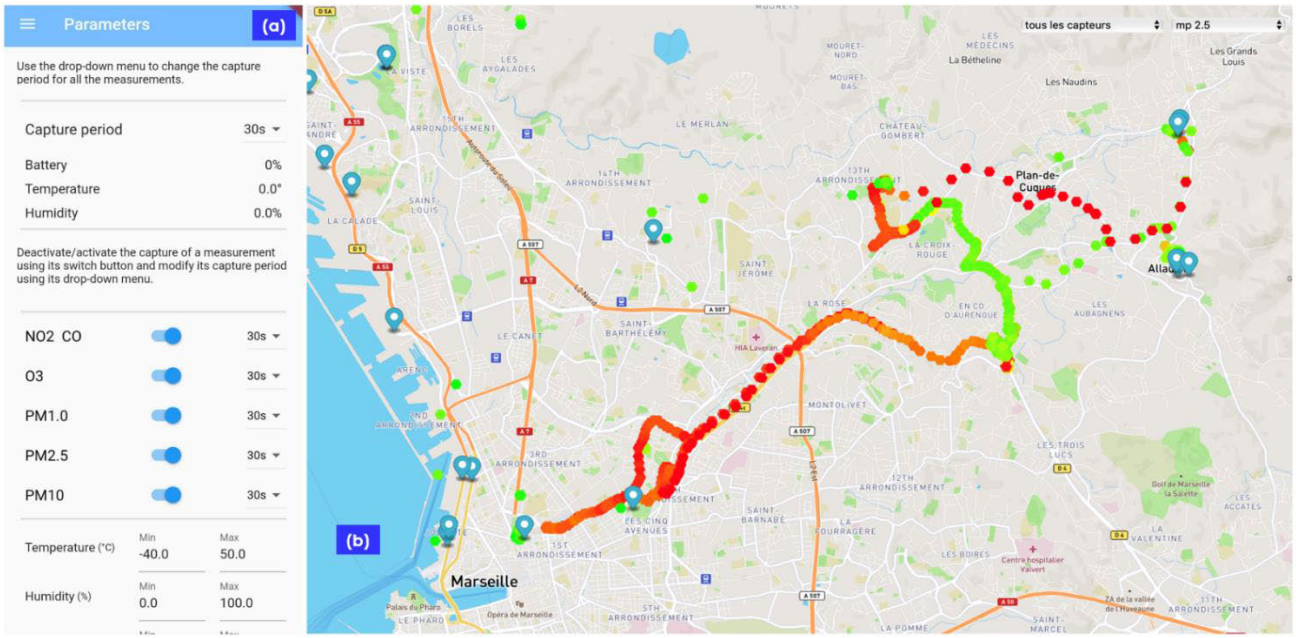

FIGURE 3. (a) Mobile application interface and (b) server-side filtered data visualization (map in French) with gas concentrations provided at the street level.

PM2.5 measurement concentration results obtained in the city of Marseille. The color code ranges from green (0 μg/m^3) to red (35 μg/m^3). These limit values are implemented on the server side.

IV. AQM SYSTEM VALIDATION

Different prototypes of AQM devices were tested in a laboratory climatic chamber for validation. The obtained results including the calibration are examined in this section.

A. FACTORY CALIBRATION

Temperature and humidity can significantly affect the accuracy of measurements in mobile monitoring systems, especially when it comes to pollutants. To implement a compensation scheme, a formula specific to each sensor is typically used which considers the sensor concentration sensitivity to temperature and humidity. The formulas developed in this section have been derived experimentally considering four different mobile devices. Before establishing the compensation formulas, the S17006 temperature and humidity rate (HR) sensor is consistency evaluated.

1) S17006 HR AND TEMPERATURE CALIBRATION

The temperature and HR sensor accuracies are ±1°C and 5%. To conduct the calibration, the PCB is placed inside a calibrated environmental chamber presented in Fig. 4 which acts as a reference instrument [41].

FIGURE 4. Temperature and humidity sensors characterization in a climatic chamber (❶ Smile device, ❷ battery, ❸ climatic chamber and ❹ reference instrument).

The measurements are made with the card outside its casing for practical wiring reasons. However, it is important to note that the casing has been designed to allow the airflow to pass through it as much as possible. The card is powered by two batteries to reproduce the actual conditions of use. The temperature and humidity setpoint values are provided by the reference chamber: the climatic chamber temperature is changing from 10°C to 40°C with 5°C step and the climatic chamber HR is changing from 10% to 70% with a 20% step. These values are referred to as Temperature reference and Humidity rate reference respectively in Fig. 5. After stabilization, the temperature and humidity values provided by the 4 considered mobile sensor devices are recorded and compared to the setpoint values to compute the error. The evolution of the temperature (Fig. 5(a)) and HR (Fig. 5(b)) errors is shown with respect to the variations of the humidity setpoint levels for the 4 devices. It can be observed that the temperature differences remain stable around 2°C and the average HR difference is around 6%. To compensate for these differences, formulas (1) and (2) have been implemented for each device.

$$T_{comp} = T_{raw} + T_{Offset} \quad (1)$$

$$HR_{comp} = HR_{raw} + HR_{Offset} \quad (2)$$

where (T_{comp}, HR_{comp}) and (T_{raw}, HR_{raw}) represent the compensated and directly measured temperature and HR, respectively. Table 2 shows the different offsets computed for each device and integrated at the device firmware level.

TABLE 2. Temperature and HR compensation offset.

Tested device	T_{Offset} (°C)	HR_{Offset} (%)
Device 1	-1.9	5.6
Device 2	-2.4	6.6
Device 3	-2.2	6.2
Device 4	-1.9	5.8

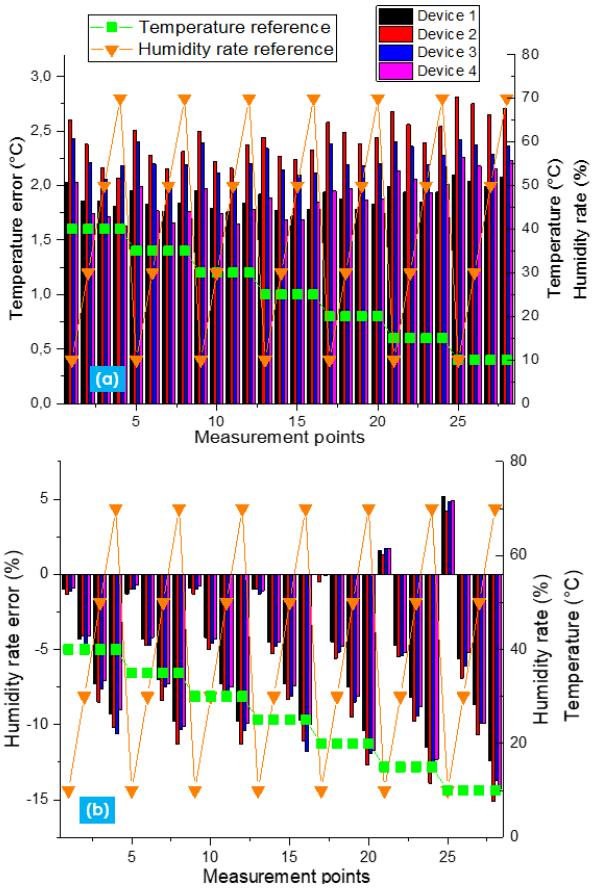

FIGURE 5. (a) Temperature and (b) HR measured errors withrespect to reference curves before compensation for 4different devices.

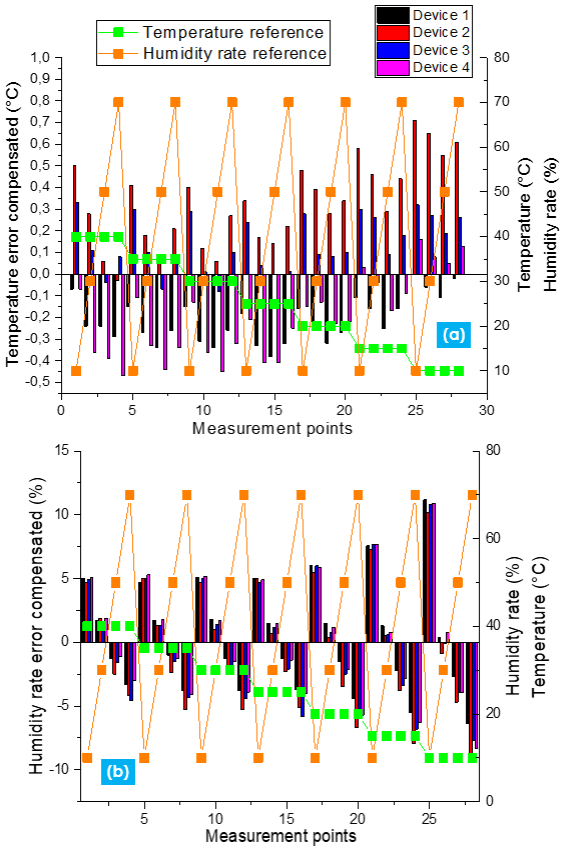

FIGURE 6. (a) Temperature and (b) HR measured errors withrespect to reference curves after compensation for 4 differentdevices.

The application of the compensation formulas for the 4 considered devices results is Fig. 6(a)-(b) where the sensor temperature and HR values are compensated. The average temperature error is maintained below 0.23°C and the HR one below 3.77%.

2) NITROGEN DIOXIDE (MICS6814)

A compensation formula is defined to track the NO_2 concentration changes according to temperature and HR variations as seen in Fig. 7. The formula is based on a matrix of different pairs of temperature and HR values. For different setpoint pairs (temperature, HR), the NO_2 concentration is measured. The temperature step is set to 5°C (green curve) and the HR step is set to 20 % (orange curve).

The NO_2 raw concentration is expressed in ADU (Analog to Digital Converter (ADC) Unit) corresponding to the voltage at the sensor output measured by the microcontroller ADC. The ADU value is given by:

$$ADU = \frac{ADC_{\max} V_{out}}{V_0} \tag{3}$$

where V_{out} and ADU represent the sensor output voltage and the ADC result, respectively. $V_0 = 3.3$ V and $ADC_{max} = 4095$ correspond to the ADC reference voltage and the ADC full-scale range (for a 12-bit ADC), respectively. From the

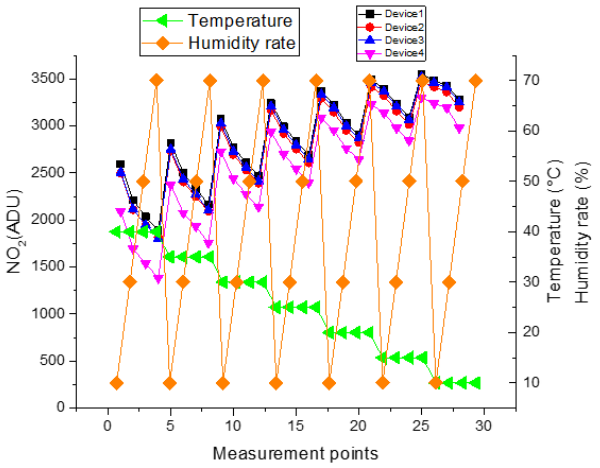

FIGURE 7. Evolution of the NO_2 concentration versus temperature and HR for 4 devices.

NO_2 concentration measurement matrix, the generic compensation formula is expressed in (4). Equation (4) parameters are provided in (5).

$$ADU_{NO_2comp} = ADU_{NO_2raw} + c_{h1} HR_{comp}^2 + c_{h2} HR_{comp} + c_{h3} \tag{4}$$

with:

$$\begin{cases} c_{h1} = a_1 T_{comp}^2 - b_1 T_{comp} + c_1 \\ c_{h2} = a_2 T_{comp}^2 + b_2 T_{comp} - c_2 \\ c_{h3} = a_3 T_{comp}^2 - b_3 T_{comp} - c_3 \end{cases} \tag{5}$$

where ADU_{NO_2comp} represents the compensated NO_2 concentration, ADU_{NO_2raw} represents the measured concentration, and T_{comp} and HR_{comp} are the compensated temperature and HR parameters, respectively. According to (4), the compensated NO_2 concentration includes the raw one added to a polynomial regression expression accounting for the temperature and HR parameters. In (6) and (7), the ADU image is converted into actual NO_2 concentrations in ppm.

$$NO_2(ppm) = \frac{ratio_{NO_2}^{\alpha}}{\beta} \tag{6}$$

with:

$$ratio_{NO_2} = \frac{ADU_{NO_2}}{ADU0_{NO_2}} \tag{7}$$

where $\alpha = 1.007$ and $\beta = 6.855$ are coefficients supplied by the sensor manufacturer, ADU_{NO2} is the compensated ADU measurement and $ADU0_{NO2}$ is the measurement after the initial laboratory calibration.

3) CARBON MONOXIDE (MICS6814)

The above-mentioned temperature and humidity compensation process is repeated for CO concentrations (i.e., the same matrix of temperature and HR pairs is used). The evolution of the concentration of CO for different temperatures and HR values is presented in Fig. 8. Temperature ranging from 10°C

to 40°C (green curve) and HR ranging from 10% to 70% (orange curve).

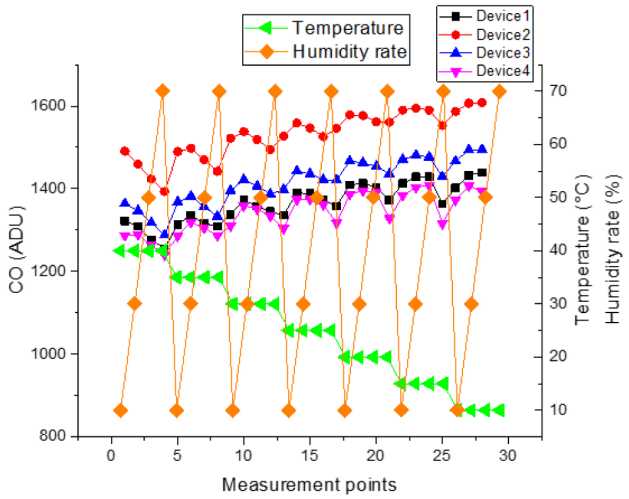

FIGURE 8. Evolution of the CO concentration versus temperature and humidity.

Based on Fig. 8, the extracted compensation formula is given by (8):

$$ADU_{COcomp} = ADU_{COraw} + c_{h1}HR_{raw}^2 + c_{h2}HR_{raw} + c_{h3} \tag{8}$$

where ADU_{COcomp} and ADU_{COraw} are the compensated and raw CO concentrations, respectively. According to (8), the compensated CO concentration is made of the raw one added to a polynomial regression to compensate for temperature and humidity variations. Finally, the CO concentration in ppm is given by:

$$CO(ppm) = \frac{ADU_{COcomp} - ADU0_{CO}}{\theta + \frac{T_{comp}-\zeta}{\eta}} \tag{9}$$

where ADU_{COcomp} is the compensated CO concentration digital image, $\zeta = 20$, $\eta = 10$ and θ are coefficients supplied by the manufacturer, $ADU0_{CO}$ is the measurement after the initial laboratory calibration. Note that the proposed calibration focuses on compensating for the effects of temperature and humidity. Issues related to poisoning and drift are not addressed.

B. DEVICE CO-LOCATION TESTS IN A CONTROLLED ENVIRONMENT

To rigorously assess the sensor system precision across various pollutants in controlled indoor environments, a series of tests involving co-located devices has been conducted. A warm-up period tailored to each gas sensor is essential before taking measurements. This step ensures that both the sensors and the climatic chamber are fully operational.

1) CARBON MONOXIDE (MICS6814)

In CO co-location tests, two compensated sensors are placed within the same indoor setting. After CO gas injection, Fig. 9(a) and Fig. 9(b) confirm an excellent correlation between the two CO concentrations. In Fig. 9(a), the two considered devices show the same trend for varying CO concentrations measured during 700 s.

In addition, the correlation curve plotted presented in Fig. 9(b) shows that the two-device concentrations are well correlated. Indeed, if we use the coefficient of determination (R^2) as the parameter of interest, we obtain a curve close to the $y = x$ curve with $R^2 = 0.992$.

2) NITROGEN DIOXIDE (MICS6814)

The co-location test method employed for CO concentration is similarly applied to NO2 concentration. The co-location test results presented in Fig. 10(a) indicate that, for two different devices within the test window of 1400 to 2400 seconds, the NO_2 concentrations exhibit the same trend. In addition, the correlation curve presented in Fig. 10(b) shows that the two device concentrations are well correlated with $R^2 = 0.995$.

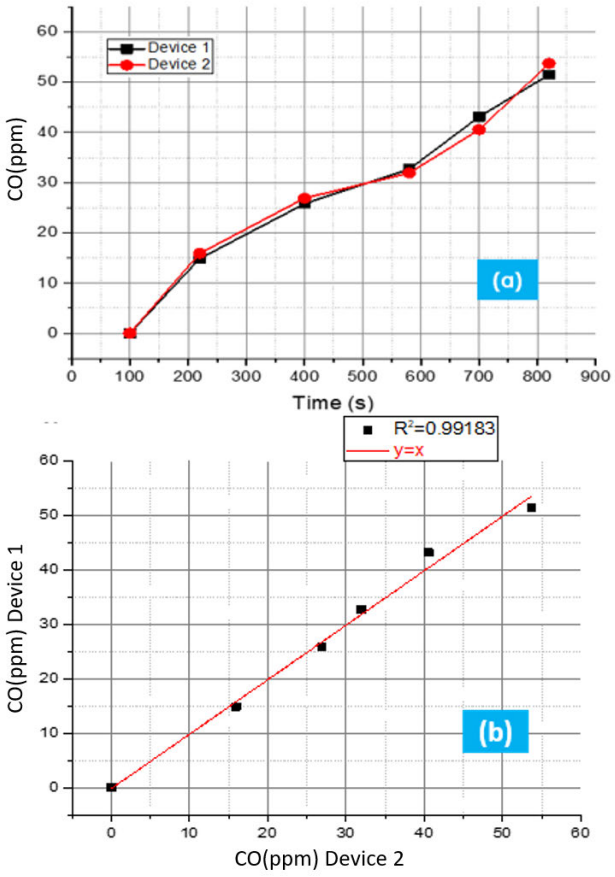

FIGURE 9. (a) Evolution of CO concentration during a gas injection test for 2 different devices and (b) correlation curve.

3) OZONE (ZMOD4510) AND AQI (ZMOD4510)

Like its predecessors, the O_3 sensor test results are very encouraging. The two tested devices' trend is similar with

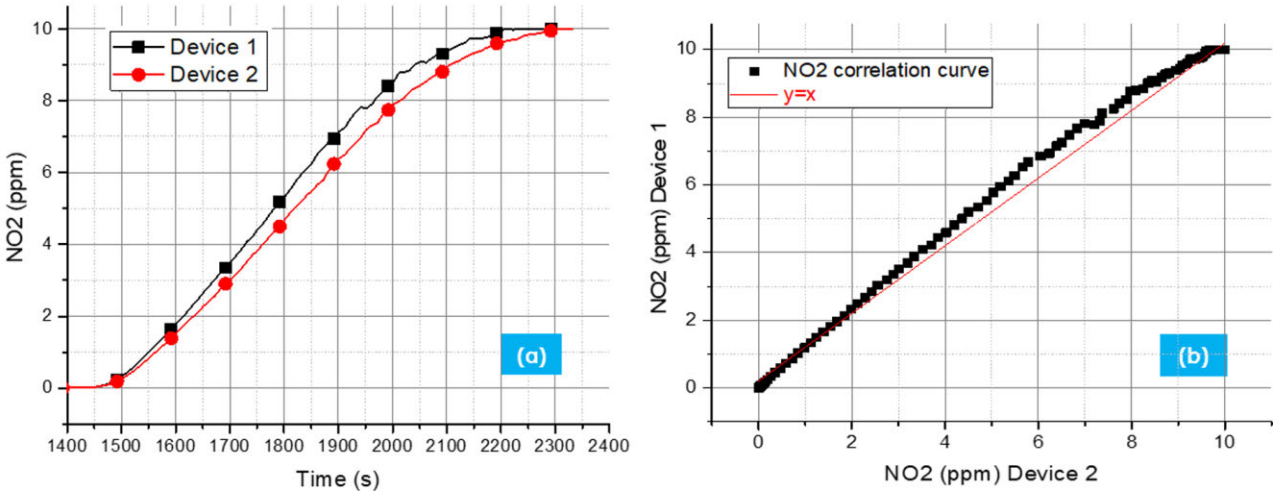

FIGURE 10. (a) Evolution of the NO_2 concentration during a gas injection test for 2 different devices and (b) correlation curve.

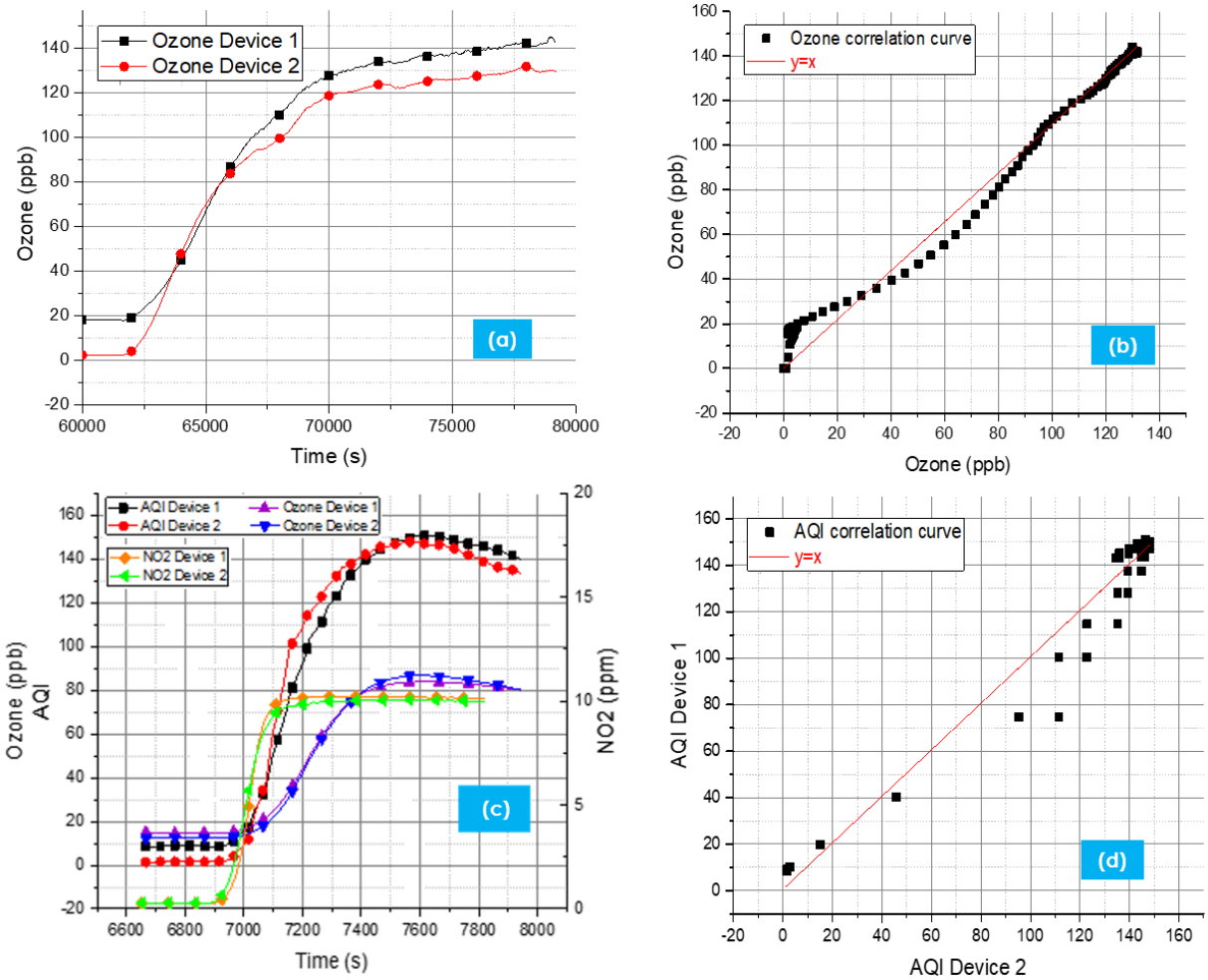

FIGURE 11. Evolution of (a) O_3 concentration during a gas injection test and (b) correlation curve. (c) AQI index evaluation during a gas injection test and (d) correlation curve.

the exception of an offset for high and low concentrations as seen in Fig. 11(a). The strong correlation between the two devices presented in Fig. 11(b) is supported by an R^2 value of 0.956. The AQI indicates the overall state of air pollution. The higher the level of air pollution, the higher the AQI. To assess the sensor system's effectiveness in calculating the AQI, two

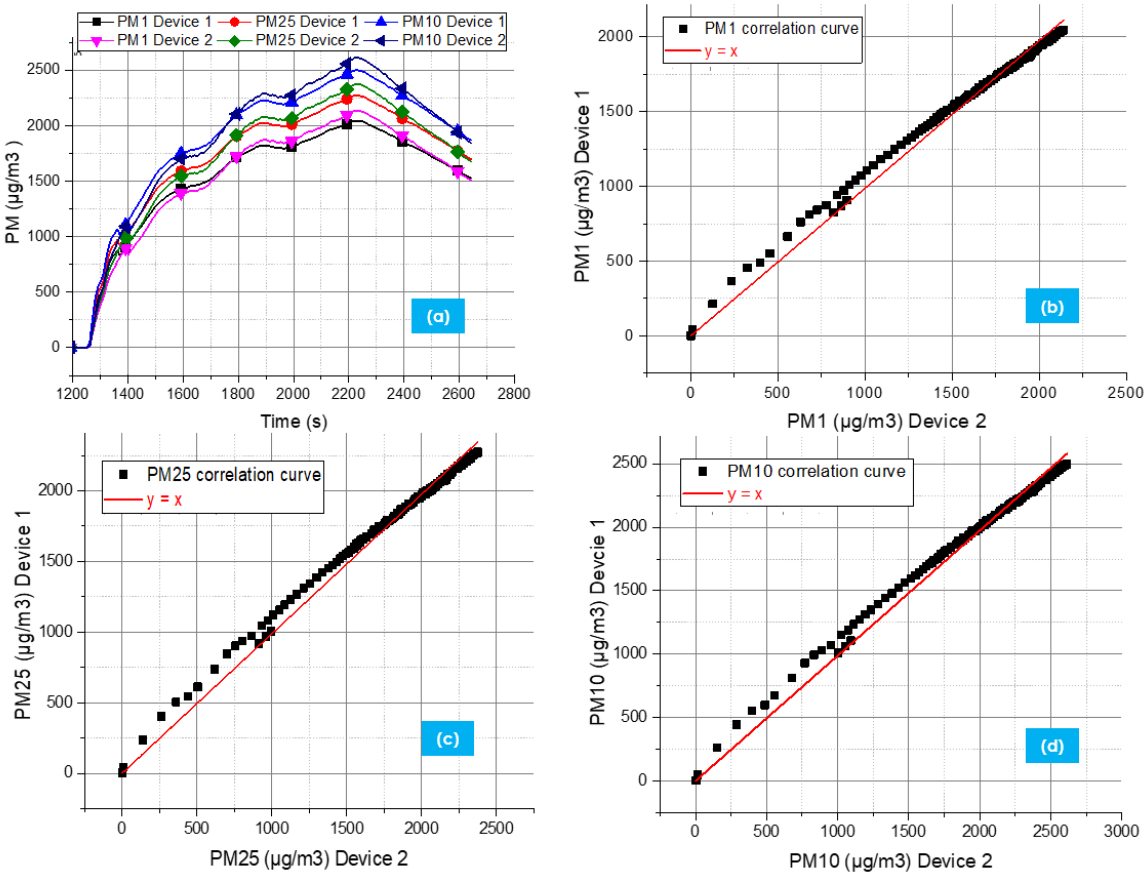

FIGURE 12. (a) Evolution of PM concentrations during particulate injection tests for 2 co-located devices, correlation curve for (b) PM1, (c) PM2.5 and (d) PM10.

co-located sensor concentrations are compared during NO_2 and O_3 injection. In Fig. 11(c), the AQI parameter evolution is plotted versus the O_3 and NO_2 concentration variations. Fig. 11(d) shows that these variations have a direct impact on the AQI value. Additionally, the AQI correlation line is once again compared to the y = x curve. With an $R^2 = 0.98$, the results are consistent across the two devices.

4) MICROPARTICLES (PM3015)

For PMs (PM1, PM2.5 and PM10), co-located sensors are tested using a nebulizer to diffuse particles. Fig. 12(a) shows that the PM concentrations exhibit similar trends pairwise. The correlation curves depicted in Fig. 12(b), 12(c) and 12(d) are once again consistent according to the R^2 parameter. R^2 results are summarized in Table 3. The PM sensors utilized in this study demonstrate a strong correlation, with R^2 values greater than 0.99.

TABLE 3. R^2 coefficient of PM1, PM2.5 and PM1.

PM1	PM2.5	PM10
0.99875	0.99875	0.99875

C. DEVICE AUTONOMY EVALUATION

An experimental characterization was performed to quantify the battery autonomy. AQM devices 1 and 2 were considered for the test protocol depicted in Fig. 13(a). An Arduino board connected to the AQM device is used to monitor the battery voltage over time and the smartphone terminal is used to display the battery autonomy evolution. In Fig. 13(b), we observe that the tested devices' battery discharge took 28 h, with all the sensors of the AQM activated along with a sampling time of 30 seconds.

V. OUTDOOR TEST AND COMPARISON WITH REFERENCE STATIONS

In addition to laboratory tests, the following section evaluates the AQM device in real-world conditions in the city of Marseille, France.

A. CONTEXT

To conduct our experiment, we have first selected a route in the city of Marseille, which includes locations of air quality monitoring stations equipped with reference instruments (Fig. 14). The air quality was monitored at 30 second intervals throughout the walking journey. As we approached within 2 meters of one of the four monitoring stations (Place Verneuil, Longchamps, Jean Moulin (which does not measure PM2.5) and Rabatau), we compared the measurements from our AQM device with those from the reference instruments.

TABLE 4. Comparison of Gas and AQM sensor performances.

Device Name	Measured Pollutants	Power Source	Accuracy (R^2 or others)	Size	Special Features
AirVisual Pro [42]	PM2.5, PM10, CO_2, Temp, RH	Battery/AC	$R^2 = 0.95$ for PM2.5	10.16 x 18.42 x 8.26 cm	Cloud data storage, mobile app
PurpleAir PA-II [43]	PM2.5, PM10	AC	$R^2 = 0.92$ for PM2.5	8.5×12.5 cm	High data granularity, open API
Aeroqual Series 300 [44]	O_3, NO_2, CO, VOCs	Battery/AC	$R^2 = 0.90$ for NO_2	19.5 x 12.2 x 5.4 cm	Swappable sensor heads
Temtop M10 [45]	PM2.5, HCHO (formaldehyde), VOCs	Battery	$R^2 = 0.88$ for PM2.5	8.2 x 8.2 x 3.1 cm	Low-cost, portable
Our work	PM1, PM2.5, PM10, O_3, NO_2, CO, AQI, Temp, RH	Battery/AC	$R^2 = 0.91$ for PM2.5 and 0.93 for O_3	3.5 x 4.7 x 3.5 cm	Cloud data storage, mobile app, Low-cost, portable

This comparison was conducted during a 30 minutes stop at each station.

B. PM2.5 WALK-MOVEMENT RESULTS

The first experimentation involves conducting walk-movement tests around four air quality stations acting as reference instruments and labeled with yellow markers in Fig. 14. It was determined that the most relevant pollutants to monitor in these sites are PM2.5 (i.e., sites with high traffic areas and construction sites). Fig. 15 shows the comparison between PM2.5 concentrations of the mobile sensor (30 seconds sampling time) and the concentrations of three different stations during a 10,000 s walk time. The comparison shows similar concentrations when the mobile sensor is close to the reference stations (less than 5 meters). Pollution peaks up to 80 $\mu g/m^3$ are also detected due to occasional events such the proximity of trucks, smokers, etc. The obtained results highlight a good indicator of AQ for concentrations lower than 10 $\mu g/m^3$ in Marseille urban area.

C. OZONE AND PM2.5 STATIC EXPERIMENTAL RESULTS

The second experiment considers a static test conducted close to an easily accessible reference station. O_3 an PM2.5 concentrations were measured every 30 seconds by the multi-sensor device. For the fixed stations (Marseille Longchamps), the particle concentration average was recorded every 15 minutes.

Measurement results were recorded for more than 14,000 seconds. PM2.5 and O_3 concentrations are plotted in Fig. 16(a) and Fig. 16(b) respectively where the mobile device concentrations are compared with the fixed station (referred to as ''Longchamps'') concentrations. The concentrations measured by the reference station show strong agreement with those recorded by the mobile sensor, achieving a R^2 score of 0.91 for PM2.5 and 0.93 for O_3. Also, it is worth mentioning that concentration peaks are also detected due to specific events (Parc Longchamps gardener's break).

D. COMPARISON WITH STATE-OF-THE-ART AQ DEVICES

The innovative aspect of the proposed AQ device can be highlighted through a comparison with existing research studies [42], [43], [44], [45]. Based on Table 4, we can state that the developed AQ device is innovative in terms of:

- The number of addressed pollutants: NO_2, CO, O_3, AQI, PM1, PM2.5, and PM10,
- Compacity,
- Mobility and portability for end-user citizens,
- Battery lifetime (can last one day),
- Accuracy.

In addition, the AQ device is promising for potential applications to be explored in the continuation of the present study (e.g., monitoring of pollution data related to industrial sites).

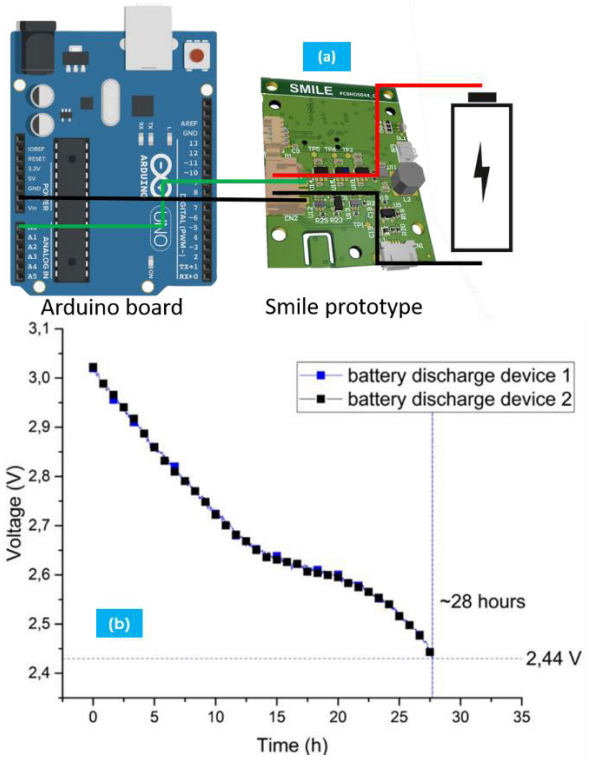

FIGURE 13. (a) AQM device autonomy test protocol and (b) battery discharge results.

VI. POLICY, CITIZEN, AND PUBLIC HEALTH IMPACT

The SMILE project, with its ability to provide detailed data on local air quality, could play a key role in shaping public policies and raising citizen awareness in the PACA (Provence-Alpes-Côte d'Azur) region. For instance,

FIGURE 14. Selected route in the city of Marseille for real-field urban tests.

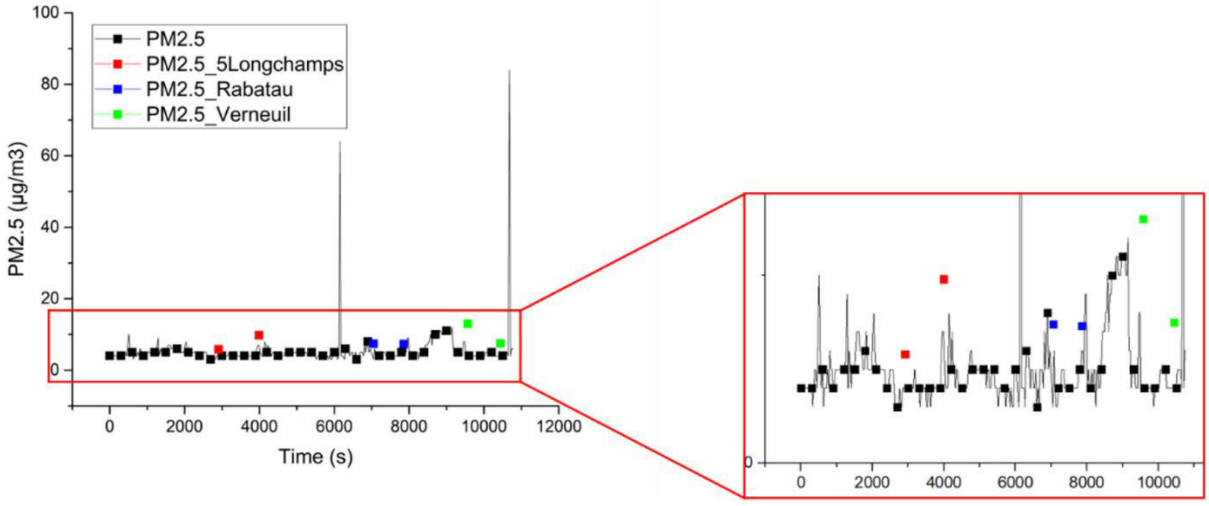

FIGURE 15. Evolution of PM2.5 concentrations during walking tests versus reference sites indicated in Fig. 14.

in addition to initiatives led by AtmoSud, the regional air quality observatory agency in charge of reference stations, SMILE's data could help refine the implementation of low-emission zones (LEZ) in cities like Marseille and Nice by identifying pollution hotspots that are not currently well monitored. At the same time, by making SMILE's data available to a large public through its dedicated application and online platform, SMILE could empower citizens to better understand air quality issues and act to protect both their health and the environment. For instance, citizens could use air quality information to avoid high-risk areas or times of day when pollution levels are at their peak. Additionally, on the public health side, SMILE's data could be combined with local health statistics to identify areas with higher respiratory risks, supporting targeted prevention campaigns in collaboration with regional health agencies.

VII. CONCLUSION

Air pollution, closely intertwined with daily life and global climate change, is a pressing concern for citizens and urban environments worldwide. In response to this challenge, the SMILE project, whose research work results are described in this paper, proposes a low-cost, mobile, and connected sensor device designed to provide street-level AQ data. The hardware and software design implementation of an innovative AQM devices is developed. A dedicated mobile application provides instant access to AQ data in the form of street-level mappings, offering geo-localized information. The device

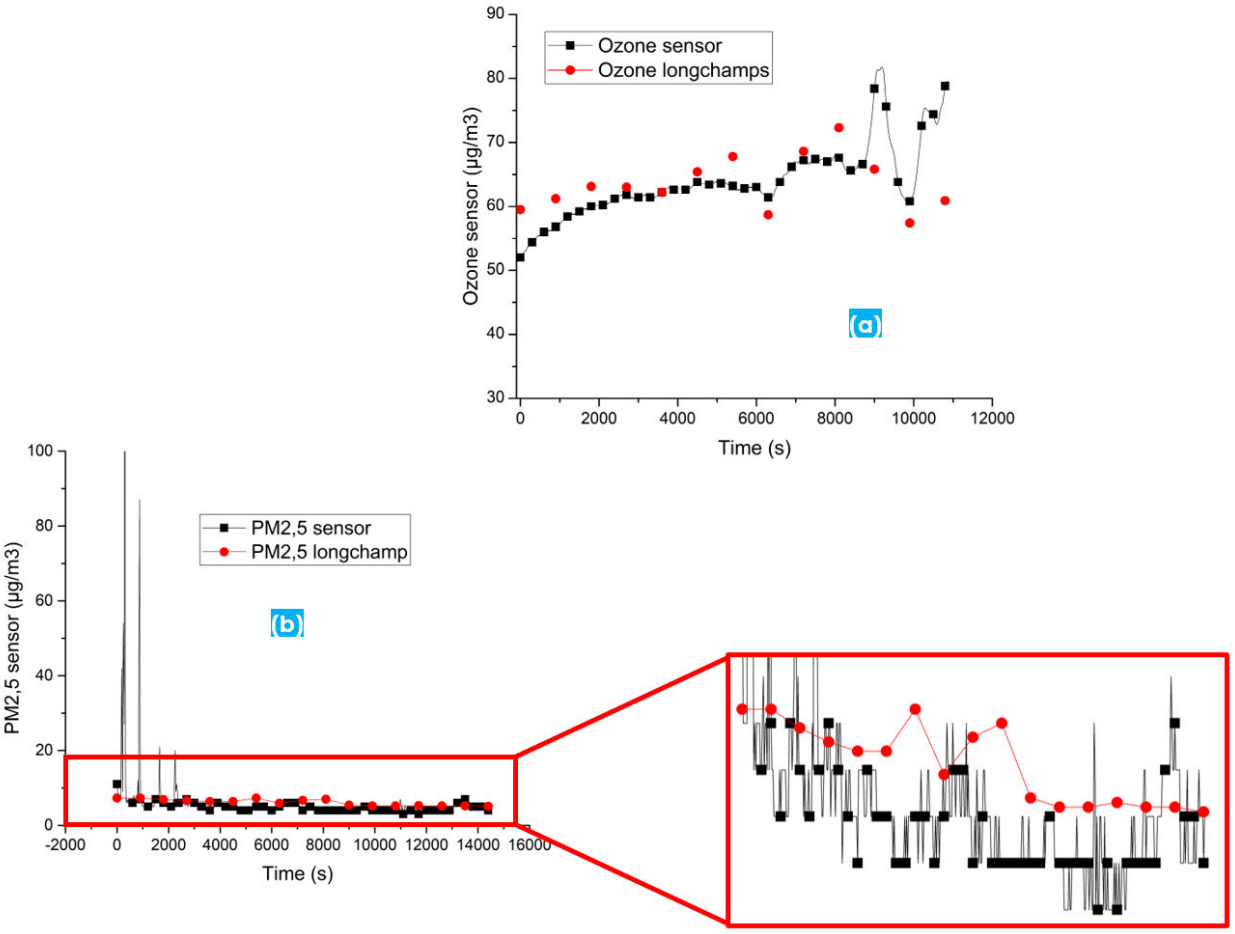

FIGURE 16. Comparison of (a) O_3 and (b) PM2.5 particulate concentrations with the Parc Longchamps reference site.

targets key reactive gases including pollutants such as NO_2, O_3, and CO, as well as PM in three size classes (e.g., PM1, PM2.5 and PM10). From a technical standpoint, the proposed AQM device was calibrated in a laboratory test room offering temperature and humidity control. The reliability of the sensor system has been assessed using two approaches: sensor-to-sensor correlation results and comparison of the sensor results with those provided by a reference instrument. The evaluation demonstrated a strong correlation across various pollutants tested for co-located sensors, with particularly good results for PM. Real-world urban environment experiments were carried out by comparing the sensor data with reference stations in Marseille city. The results appeared to be well correlated between the reference instruments and the AQM devices. The developed AQM device is also innovative due to its ability to monitor different types of pollutants, along with its optimal design, portability, autonomy, and real-time data monitoring capability at an affordable cost (less than $90).

REFERENCES

[1] R. B. Schlesinger, "The health impact of common inorganic components of fine particulate matter ($PM_{2.5}$) in ambient air: A critical review," *Inhalation Toxicol.*, vol. 19, no. 10, pp. 811–832, Jan. 2007, doi: 10.1080/08958370701402382.

[2] P. Breitegger and A. Bergmann, "Air quality and health effects—How can wireless sensor networks contribute? A critical review," in *Proc. Int. Conf. Broadband Commun. Next Gener. Netw. Multimedia Appl. (CoBCom)*, Sep. 2016, pp. 1–8, doi: 10.1109/COBCOM.2016.7593507.

[3] Y. Lu and T. B. Fang, "Examining personal air pollution exposure, intake, and health danger zone using time geography and 3D geovisualization," *ISPRS Int. J. Geo-Inf.*, vol. 4, no. 1, pp. 32–46, Mar. 2015, doi: 10.3390/ijgi4010032.

[4] J.-B. Garrocq and S. Parasie, "Peut-on redistribuer la surveillance de la qualité de l'air? Une enquête sur les métrologies à l'œuvre dans un concours institutionnel d'évaluation de micro-capteurs," *Revue d'anthropologie des Connaissances*, vol. 16, no. 4, p. 16, Dec. 2022, doi: 10.4000/rac.29150.

[5] M. V. Narayana, D. Jalihal, and S. M. S. Nagendra, "Establishing a sustainable low-cost air quality monitoring setup: A survey of the state-of-the-art," *Sensors*, vol. 22, no. 1, p. 394, Jan. 2022, doi: 10.3390/s22010394.

[6] T. Jin and F. Bouthillier, "Facilitating access to information through collaboration: Examination of the role of collaborative technology in competitive intelligence," in *Proc. Annu. Conf. CAIS/Actes du Congrès Annuel de (l'ACSI)*, 2004, pp. 1–14, doi: 10.29173/cais326.

[7] M. Marć, M. Tobiszewski, B. Zabiegała, M. de la Guardia, and J. Namieśnik, "Current air quality analytics and monitoring: A review," *Analytica Chim. Acta*, vol. 853, pp. 116–126, Jan. 2015, doi: 10.1016/j.aca.2014.10.018.

[8] Y. Robin, J. Amann, T. Schneider, A. Schütze, and C. Bur, "Comparison of transfer learning and established calibration transfer methods for metal oxide semiconductor gas sensors," *Atmosphere*, vol. 14, no. 7, p. 1123, Jul. 2023, doi: 10.3390/atmos14071123.

[9] S. Messan, A. Shahud, A. Anis, R. Kalam, S. Ali, and M. I. Aslam, "Air-MIT: Air quality monitoring using Internet of Things," *Eng. Proc.*, vol. 20, no. 1, p. 45, 2022, doi: 10.3390/engproc2022020045.

[10] S. Mahajan, J. Gabrys, and J. Armitage, "AirKit: A citizen-sensing toolkit for monitoring air quality," *Sensors*, vol. 21, no. 12, p. 4044, Jun. 2021, doi: 10.3390/s21124044.
[11] V. E. Alvear-Puertas, Y. A. Burbano-Prado, P. D. Rosero-Montalvo, P. Tözün, F. Marcillo, and W. Hernandez, "Smart and portable air-quality monitoring IoT low-cost devices in ibarra city, Ecuador," *Sensors*, vol. 22, no. 18, p. 7015, Sep. 2022, doi: 10.3390/s22187015.
[12] M. Penza, D. Suriano, V. Pfister, M. Prato, and G. Cassano, "Urban air quality monitoring with networked low-cost sensor-systems," *Proceedings*, vol. 1, no. 4, p. 573, 2017, doi: 10.3390/proceedings1040573.
[13] P. Diviacco, M. Iurcev, R. J. Carbajales, N. Potleca, A. Viola, M. Burca, and A. Busato, "Monitoring air quality in urban areas using a vehicle sensor network (VSN) crowdsensing paradigm," *Remote Sens.*, vol. 14, no. 21, p. 5576, Nov. 2022, doi: 10.3390/rs14215576.
[14] A. Géczy, L. Kuglics, L. Jakab, and G. Harsányi, "Wearable smart prototype for personal air quality monitoring," in *Proc. IEEE 26th Int. Symp. Design Technol. Electron. Packag. (SIITME)*, Oct. 2020, pp. 84–88, doi: 10.1109/SIITME50350.2020.9292309.
[15] T. H. Frampton, A. Tiele, and J. A. Covington, "Development of a personalised environmental quality monitoring system (PONG)," *IEEE Sensors J.*, vol. 21, no. 13, pp. 15230–15236, Jul. 2021, doi: 10.1109/JSEN.2021.3073752.
[16] F. Mazumder, P. Goswami, T. Toha, A. Mondol, and S. Alam, "Towards developing a smart air quality monitoring and security system to ensure workplace health and safety," in *Proc. Int. Conf. 4th Ind. Revolution Beyond* Dec. 2021, pp. 291–303, doi: 10.1007/978-981-19-2445-3_19.
[17] D. Lohani, A. Barthwal, and D. Acharya, "Modeling vehicle indoor air quality using sensor data analytics," *J. Reliable Intell. Environ.*, vol. 8, no. 2, pp. 105–115, Jun. 2022, doi: 10.1007/s40860-021-00137-2.
[18] S. Palomeque-Mangut, F. Meléndez, J. Gómez-Suárez, P. Arroyo, J.-I. Suárez, S. Frutos-Puerto, and J. Lozano, "Electronic system for citizens' air quality mapping," in *Proc. IEEE Sensors*, Oct. 2021, pp. 1–4, doi: 10.1109/SENSORS47087.2021.9639578.
[19] D. E. Williams, "Low cost sensor networks: How do we know the data are reliable?" *ACS Sensors*, vol. 4, no. 10, pp. 2558–2565, Oct. 2019, doi: 10.1021/acssensors.9b01455.
[20] B. Potter, G. Valentino, L. Yates, T. Benzing, and A. Salman, "Environmental monitoring using a drone-enabled wireless sensor network," in *Proc. Syst. Inf. Eng. Design Symp. (SIEDS)*, Apr. 2019, pp. 1–6, doi: 10.1109/SIEDS.2019.8735615.
[21] P. Gajbhiye and A. Mahajan, "A survey of architecture and node deployment in wireless sensor network," in *Proc. 1st Int. Conf. Appl. Digit. Inf. Web Technol. (ICADIWT)*, Aug. 2008, pp. 426–430, doi: 10.1109/ICADIWT.2008.4664386.
[22] S. Palomeque-Mangut, F. Meléndez, J. Gómez-Suárez, S. Frutos-Puerto, P. Arroyo, E. Pinilla-Gil, and J. Lozano, "Wearable system for outdoor air quality monitoring in a WSN with cloud computing: Design, validation and deployment," *Chemosphere*, vol. 307, Nov. 2022, Art. no. 135948, doi: 10.1016/j.chemosphere.2022.135948.
[23] R. Kingsy Grace and S. Manju, "A comprehensive review of wireless sensor networks based air pollution monitoring systems," *Wireless Pers. Commun.*, vol. 108, no. 4, pp. 2499–2515, Oct. 2019, doi: 10.1007/s11277-019-06535-3.
[24] S. De Vito, E. Esposito, E. Massera, F. Formisano, G. Fattoruso, S. Ferlito, A. Del Giudice, G. D'Elia, M. Salvato, T. Polichetti, P. D'Auria, A. M. Ionescu, and G. Di Francia, "Crowdsensing IoT architecture for pervasive air quality and exposome monitoring: Design, development, calibration, and long-term validation," *Sensors*, vol. 21, no. 15, p. 5219, Jul. 2021, doi: 10.3390/s21155219.
[25] M. J. Fadhil, S. K. Gharghan, and T. R. Saeed, "Air pollution forecasting based on wireless communications: Review," *Environ. Monitor. Assessment*, vol. 195, no. 10, p. 1152, Sep. 2023, doi: 10.1007/s10661-023-11756-y.
[26] O. Robert, M. M. Rahman, H. Kiyoshi, A. Shrestha, and A. Vaseashta, "SnO_2 gas sensors and geo-informatics for air pollution monitoring," *J. Optoelectron. Adv. Mater.*, vol. 13, pp. 560–564, May 2011.
[27] H. Tariq, A. Abdaoui, F. Touati, M. A. E. Al-Hitmi, D. Crescini, and A. B. Mnaouer, "An autonomous multi-variable outdoor air quality mapping wireless sensors IoT node for Qatar," in *Proc. Int. Wireless Commun. Mobile Comput. (IWCMC)*, Doha, Qatar, Jun. 2020, pp. 2164–2169, doi: 10.1109/IWCMC48107.2020.9148392.
[28] F. Corno, E. Guercio, L. Russis, and E. Gargiulo, "Designing for user confidence in intelligent environments," *J. Reliable Intell. Environ.*, vol. 1, pp. 11–21, Jul. 2015, doi: 10.1007/s40860-015-0001-7.
[29] L. Capezzuto, L. Abbamonte, S. De Vito, E. Massera, F. Formisano, G. Fattoruso, G. Di Francia, and A. Buonanno, "A maker friendly mobile and social sensing approach to urban air quality monitoring," in *Proc. IEEE SENSORS*, Nov. 2014, pp. 12–16, doi: 10.1109/ICSENS.2014.6984920.
[30] *Some Basic Consideration in the Design of an Air Pollution Monitoring System*. Accessed: Jan. 8, 2024. [Online]. Available: https://www.tandfonline.com/doi/epdf/10.1080/00022470.1971.10469574?needAccess=true
[31] *BMD-360_DataSheet_UBX-19039466.PDF*. Apr. 16, 2024. [Online]. Available: https://content.u-blox.com/sites/default/files/BMD-360_DataSheet_UBX-19039466.pdf
[32] *MX25R6435F, Wide Range, 64Mb, V1.6.PDF*. Accessed: Apr. 16, 2024. [Online]. Available: https://www.macronix.com/Lists/Datasheet/Attachments/8868/MX25R6435F,%20Wide%20Range,%2064Mb,%20v1.6.pdf
[33] *1143_Datasheet-MiCS-6814-Rev-8.PDF*. Accessed: Jan. 8, 2024. [Online]. Available: https://www.sgxsensortech.com/content/uploads/2015/02/1143_Datasheet-MiCS-6814-rev-8.pdf
[34] *Outdoor Air Q Pm3015 Laser Particle Sensor Module Specifications | PDF | Electronics | Electricity*. Scribd. Accessed: Jan. 8, 2024. [Online]. Available: https://www.scribd.com/document/429110264/Outdoor-Air-q-Pm3015-Laser-Particle-Sensor-Module-Specifications
[35] *REN_ZMOD4510_DST_20210630-1999508.PDF*. Accessed: Jan. 8, 2024. [Online]. Available: https://eu.mouser.com/datasheet/2/698/REN_ZMOD4510_DST_20210630-1999508.pdf
[36] *Si7006_A20-1397947.PDF*. Accessed: Jan. 8, 2024. [Online]. Available: https://eu.mouser.com/datasheet/2/368/Si7006_A20-1397947.pdf
[37] L. Rossi, J.-M. Linares, J. Chaves-Jacob, J. Mailhé, and J.-M. Sprauel, "Design optimization using statistical confidence boundaries of response surfaces: Application to robust design of a biomedical implant," *CIRP Ann.*, vol. 63, no. 1, pp. 141–144, Jan. 2014, doi: 10.1016/j.cirp.2014.03.088.
[38] J. Linares, J. Chaves-Jacob, Q. Lopez, and J.-M. Sprauel, "Fatigue life optimization for 17-4Ph steel produced by selective laser melting," *Rapid Prototyping J.*, vol. 28, no. 6, pp. 1182–1192, Jan. 2022, doi: 10.1108/RPJ-03-2021-0062.
[39] K. D. Purkayastha, R. K. Mishra, A. Shil, and S. N. Pradhan, "IoT based design of air quality monitoring system Web server for Android platform," *Wireless Pers. Commun.*, vol. 118, no. 4, pp. 2921–2940, Jun. 2021, doi: 10.1007/s11277-021-08162-3.
[40] *Flutter_Reactive_BLE | Flutter Package*. Dart Packages. Accessed: Jan. 11, 2024. [Online]. Available: https://pub.dev/packages/flutter_reactive_ble
[41] M. Gmbh and C. Kg. *DS_Memmert Climate Chamber ICH110–EN*. Accessed: Jan. 1, 2024. [Online]. Available: https://www.memmert.com/fr/produit/enceintes-climatiques/enceinte-climatique/ich110/pdf
[42] M. L. Zamora, J. Rice, and K. Koehler, "One year evaluation of three low-cost PM2.5 monitors," *Atmos. Environ.*, vol. 235, Aug. 2020, Art. no. 117615, doi: 10.1016/j.atmosenv.2020.117615.
[43] *Field Evaluation of Low-Cost PM Sensors (Purple Air PA-II) Under Variable Urban Air Quality Conditions, in Greece*. Accessed: Nov. 21, 2024. [Online]. Available: https://www.mdpi.com/2073-4433/11/9/926
[44] D. Laurinavičienė, "Ground-level ozone air pollution in Vilnius City," *Environ. Res., Eng. Manage.*, vol. 49, no. 3, pp. 21–28, Sep. 2009.
[45] P. N. deSouza, "Key concerns and drivers of low-cost air quality sensor use," *Sustainability*, vol. 14, no. 1, p. 584, Jan. 2022, doi: 10.3390/su14010584.

JONAS PELLEGRINO (Student Member, IEEE) received the engineering degree in microelectronics and telecommunications from Aix-Marseille University, in 2023. He is currently pursuing the Ph.D. degree with dual supervision with the Memory Team (MEM) and the Integrated Circuits and Systems Design Team (CCSI), CNRS-IM2NP Laboratory.

HASSEN AZIZA (Member, IEEE) received the B.S. and M.S. degrees in electrical engineering from the University of Marseille, France, and the Ph.D. degree from Aix-Marseille University, France, in 2002. He is currently an Associate Professor with the Institute of Materials, Microelectronics and Nanosciences of Provence (IM2NP), Aix-Marseille University. He is the (co-)author of more than 180 papers in international conferences and journals and is (co)inventor of five patents. He is involved in the French National Research Agency Project DIPMEM dedicated to hybrid circuit design (CMOS-ReRAM), in the regional level project SMILE dedicated to air monitoring, and is working together with CEA-LETI on Neuro-Memristive circuits. Since 2017, he has been the IM2NP's ''Memory Team'' Leader. IM2NP's ''Memory Team'' is composed of 12 permanents (four professors and eight associate professors). His research topics conducted by the group are fully dedicated to microelectronics circuit design and fabrication end tests. His research interests include the design, testing, and reliability of microelectronic circuits, including conventional (Flash/EEPROM) and emerging memory circuits (Resistive RAM).

MATHIEU GUERIN (Member, IEEE) received the Engineering degree in microelectronics and telecommunications from Polytech Marseille, in 2010, and the master's degree in integrated circuits design and the Ph.D. degree from Aix-Marseille University, in 2013. He was the Technical Leader of the Analog and Radio-Frequency Design Team, IDEMIA-StarChip, for five years. During this time, he designed chips embedded in SIM cards and contactless bank cards with biometric recognition. In 2020, he joined Aix-Marseille University as an Assistant Professor and became a member with the CCSI Team, IM2NP. His primary research interests include the design and synthesis of circuits in digital electronics. Additionally, he is involved in methods of modeling and characterizing circuits in analog electronics.

PASCAL TARANTO (Member, IEEE) is currently a Full Professor with Aix-Marseille University and the Director of the Center Gilles Gaston Granger (UMR 7304). He specialized in classical British philosophy and philosophy of the Enlightenment. He published recently *Joseph Priestley Matière et Esprit au siècle des Lumières*, Paris; *Honoré Champion, coll. Les dix-huitièmes siècles* (A. McKenna, 2020); *Priestley as an heir of Newton* (C. Wolfe & F. Wunderlich) (dir.); *Joseph Priestley, Materialism and Science of the Mind–Foundations, Controversies, Reception*; *numéro spécial de Intellectual History Review*, (2019) p. 87-107. He is also involved in funded innovation and valorization projects about participative science, such as SMILE, and the designing of collaborative platforms for research, such as LABΩ.

WENCESLAS RAHAJANDRAIBE (Member, IEEE) received the B.Sc. degree in electrical engineering from Nice Sophia Antipolis University, France, in 1996, the M.Sc. degree (Hons.) in electrical engineering from the Science Department, University of Montpellier, France, in 1998, and the Ph.D. degree in microelectronics from the University of Montpellier. In 1998, he joined the Microelectronics Department, Informatics, Robotics and Microelectronics Laboratory of Montpellier. In 2003, he joined the Microelectronic Department, Materials, Microelectronics and Nanoscience Laboratory of Provence, Marseille, France, where he was an Associate Professor. Since 2014, he has been a Professor with Aix Marseille University, where he heads the Integrated Circuit Design Group of this laboratory. He is currently a Full Professor at Aix-Marseille University. He is regularly involved in participating in and leading national and international research projects (ANR, H2020, and FP7 KIC-InnoEnergy). His research interests include AMS and RF circuit design from transistor to architectural level. His present research activity is focused on ultralow power circuit design for smart sensor interfaces and embedded electronics in bioelectronic and e-health applications, wireless systems, design techniques, and architecture for multi-standard transceivers. He is an Expert on ANR, the French Agency for Research. He has served on program committees of IEEE NEWCAS and ICECS. He has been and is a Reviewer of contributions submitted to several IEEE conferences and journals, such as ISCAS, NEWCAS, MWSCAS, ESSCIRC, ESSDERC, RFIC, and IEEE TRANSACTIONS ON CIRCUITS AND SYSTEMS—I: REGULAR PAPERS, IEEE TRANSACTIONS ON CIRCUITS AND SYSTEMS—II: EXPRESS BRIEFS, and *IET Electronics Letters*.

BLAISE RAVELO (Senior Member, IEEE) is currently an University Distinguished Full Professor with NUIST, Nanjing, China. He supervised ten Ph.D. students. He is the (co-)authors of more than 450 scientific research papers in new technologies published in international journals and conferences. His research interests include multiphysics modeling, Kron's method, RF/electronics engineering, EMC/SI/PI of printed circuit boards (PCBs), and pioneer of the negative group delay (NGD) theory, engineering and applications for RF/microwave, and sensor/control/monitoring data prediction. With international partners, he is actively involved and contributes to several international research projects. He is a member of *IET Electronics Letters* Editorial Board as an Associate Editor Circuit and a System Subject Editor. He is a member of the Scientific Technical Committee of the International Conference on Antennas and Electromagnetic Systems (AES). He is a member of research groups: URSI, GDR Ondes, and Radio Society. He is a Distinguished Best Life Scientist and ranked in the Top 2% world's scientists based on years (2020–2024) by Stanford University, USA, and Elsevier. He has Google scholar H-index(2024) = 31 and i10-index(2024) = 114.